



Radiative double-electron capture for oxygen and fluorine ions colliding with thin-foil C: Effects of multiple collisions

D. S. La Mantia ^{*}, P. N. S. Kumara, C. P. McCoy, and J. A. Tanis 
Western Michigan University, Kalamazoo, Michigan 49008, USA

 (Received 20 October 2020; accepted 9 December 2020; published 21 December 2020)

Radiative double-electron capture (RDEC), a process considered the inverse of double photoionization of ions, has been investigated for ~ 2 MeV/u fully stripped and one-electron oxygen and fluorine ions colliding with thin-foil C targets. These measurements are a follow-up to the first evidence for RDEC [A. Simon, A. Warczak, T. Elkafrawy, and J. A. Tanis, *Phys. Rev. Lett.* **104**, 123001 (2010)] in ion collisions with carbon, and to our recent observation of the process for 2.11 MeV/u $F^{9,8+}$ ions [D. S. La Mantia, P. N. S. Kumara, S. L. Buglione, C. P. McCoy, C. J. Taylor, J. S. White, A. Kayani, and J. A. Tanis, *Phys. Rev. Lett.* **124**, 133401 (2020)] in collisions with gas targets of N_2 and Ne. Coincidences between emitted photons and outgoing ions in charge states $q-2$ (the expected RDEC charge state), $q-1$, and q were recorded. Differences in coincidences with all three charge states are appreciable and are attributed to unavoidable multiple charge-changing collisions of the ions as they transverse the thin-foil target. Also, significant differences between the spectra for oxygen and fluorine are seen, despite these ions being just one atomic number apart. Cross sections for RDEC were determined and compared with previous data for thin-foil solid and gas targets as well as with theoretical calculations.

DOI: [10.1103/PhysRevA.102.060801](https://doi.org/10.1103/PhysRevA.102.060801)

Recently, we reported the results of the study of radiative double-electron capture (RDEC) for F^{9+} and F^{8+} ions incident on gas targets of N_2 and Ne [1]. These measurements provided the first real proof of RDEC in ion-atom collisions, and were a follow-up to the first evidence for RDEC in O^{8+} [2] and F^{9+} [3] ions incident on thin-foil C targets. The latter measurements, however, suffered from unavoidable multiple collisions that can change the charge state of the capturing ion following an RDEC event as it continues passage through the foil. In addition, three unsuccessful attempts [4–6] to investigate RDEC were undertaken at the GSI facility in Germany, with a mixture of foil and gas targets. The O^{8+} and F^{9+} measurements that constituted the first experimental evidence of RDEC [2,3] were done following the suggestion of Nefiodov *et al.* [7] that lower-energy, mid- Z ions may lead to larger RDEC cross sections.

RDEC occurs when two electrons are captured from a target atom to bound states of the projectile ion while simultaneously emitting a single photon [8]. Hence, RDEC can be considered the inverse of double photoionization for ion-atom collisions. The process is similar to the one-electron process of radiative electron capture (REC), in which a single electron is captured with the simultaneous emission of a single photon [9,10], considered the inverse of single photoionization. Figure 1 shows the schematics of the REC and RDEC processes, where the emitted photon energies can be derived from the conservation of energy, and are given by

$$E_{\text{REC}} = K_t + B_p - B_t + \vec{v}_p \cdot \vec{p}_{it}$$

$$E_{\text{RDEC}} = 2K_t + B_p^1 + B_p^2 - B_t^1 - B_t^2 + \vec{v}_p \cdot \vec{p}_{it}^1 + \vec{v}_p \cdot \vec{p}_{it}^2.$$

Here, K_t is the kinetic energy of each electron before capture as seen from the projectile reference frame with both electrons having the same amount of kinetic energy; B_t^1 and B_t^2 are the initial binding energies of the two electrons in the target atom, and B_p^1 and B_p^2 are the binding energies in the projectile ion to which the capture occurs (these binding energies are considered positive). The quantities \vec{v}_p and $\vec{p}_{it}^1, \vec{p}_{it}^2$ represent the velocity of the projectile ion in the laboratory frame and the intrinsic momentum of the captured electron due to its orbital motion in the target atom, respectively. In general, any target electron can be captured to the same or different bound states of the projectile with each possible transition emitting a photon of its distinct energy.

In the present work, we report the results of the study of RDEC for fully stripped and one-electron $O^{8,7+}$ and $F^{9,8+}$ ions incident on thin-foil C targets, with the expectation that charge changing of the incident ion can occur after it undergoes capture in the RDEC process and continues passage through the foil. Coincidences between emitted photons and outgoing charge states $q-2$, $q-1$, and q of the colliding ion were measured. This RDEC study differs from the previous ones with a C foil [2,3] in that coincidences are measured for incident ions having one electron, in addition to the bare projectiles, and for outgoing ions in the three final charge states $q-2$, $q-1$, and q . RDEC events are observed for all three charge states, attributed to multiple charge stripping in the C foil. Cross sections for RDEC are determined and compared with the previous results for N_2 and Ne gas targets [1] and limited results for the C foil [2,3]. The results are also compared with theoretical calculations [11] to the extent possible. Significant differences are found in the experimental cross sections between oxygen and fluorine ions, despite their differing by only one atomic number. The measured cross sections are found to

^{*}david.s.lamantia@wmich.edu

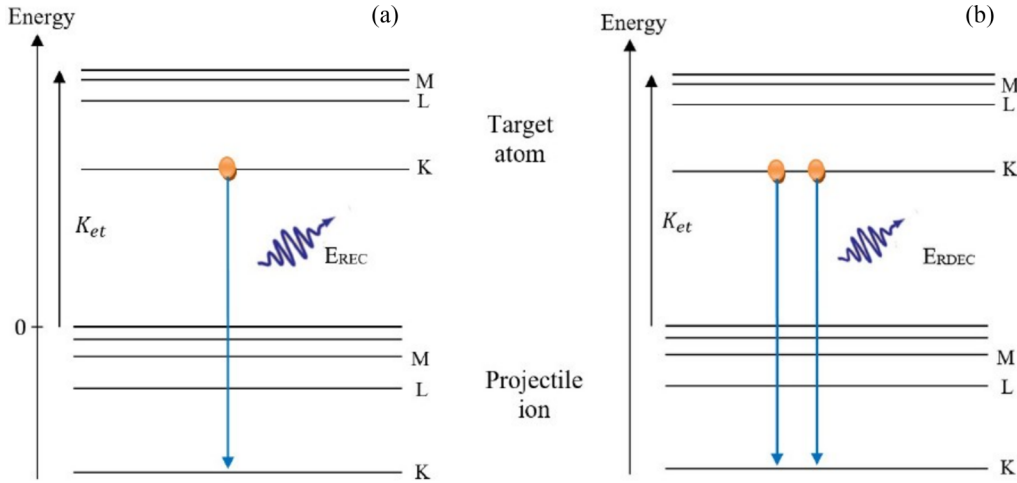


FIG. 1. Energy diagram showing the (a) REC and (b) RDEC processes. In REC, an electron is captured from a target bound state to the projectile with simultaneous emission of a single photon. In RDEC, two electrons are captured to bound states of the projectile with the simultaneous emission of a single photon. Generally, the target electrons can be captured from any bound states to any bound states of the projectile.

be roughly an order of magnitude larger than the theoretical predictions of Ref. [11].

The measurements were carried out using the 6-MV tandem Van de Graaff accelerator at Western Michigan University. Figure 2 shows a schematic of the experimental setup. The projectile ions, accelerated to ~ 2 MeV/u, collided with a thin carbon foil mounted on a holder tilted at 45° to the beam direction (the foil thickness was $10.6 \times \sqrt{2} \mu\text{g}/\text{cm}^2 = 7.53 \times 10^{17}$ atoms/cm² at this angle). A Si(Li) x-ray detector was placed at 90° to the beam as shown with no provision for changing this angle. After passing through the target, the outgoing ions were separated according to charge state using a dipole magnet, and the q-2, q-1, and q charge states were counted with separate surface-barrier detectors.

Data acquisition was accomplished in event mode with the coincidences between x rays and particles observed in the q-2, q-1, and q charge states recorded separately. This allowed the collected data to be analyzed by (1) gating the particle spectra to generate x rays associated with them (referred to as particle-gated x-ray spectra), or (2) gating the x-ray spectrum to generate the particle spectra associated with the individual charge states (referred to as x-ray-gated particle spectra).

The x-ray detector, with an effective observation area of ~ 60 mm², was positioned at a distance 2.8 cm from the target,

corresponding to a detection solid angle of 0.0765 sr. The detection efficiency of x rays with energies in the calculated RDEC energy range is greater than $\sim 98\%$. For each of the measurements with different projectiles (F^{9+} , F^{8+} , O^{8+} , and O^{7+}), short runs with an empty foil holder (i.e., without the C target) were performed in order to show that no background events contributed to the measurements.

Calculated RDEC energies of the six transitions involving transfer of at least one electron to the K shell for the four target-projectile systems are listed in Table I. For the one-electron projectiles, O^{7+} and F^{8+} , two electrons from the target atom cannot be captured to the K shell due to the existing electron in that shell. However, transitions with the final state being *KL* (corresponding to the transfer of one electron to the K shell and the other to the L shell) are possible.

Figure 3 shows the raw spectra (without applying gates) for the $\text{F}^{9+} + \text{C}$ system. The peak near channel 200 in the x-ray singles spectrum [panel (a)] is due to characteristic *F K* x rays,

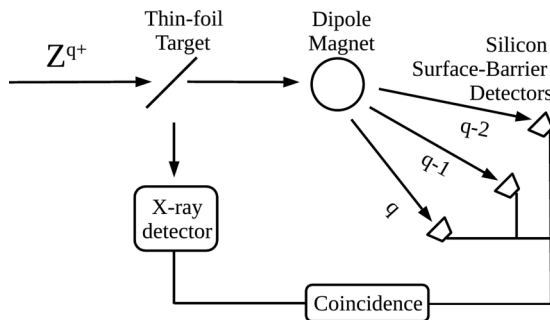


FIG. 2. Schematic diagram of the experimental setup.

TABLE I. Calculated RDEC energies (eV) for electron transitions involving at least one electron going to the projectile K shell for 2.19 MeV/u (35 MeV) $\text{O}^{8,7+}$ and 2.11 MeV/u (40 MeV) $\text{F}^{9,8+}$ ions incident on a carbon target. For the one-electron projectiles, transitions with both electrons going to the K shell are not possible due to the electron already present in that shell. *V* refers to valence (quasifree) electrons.

RDEC electron transition	Projectile-target system			
	35 MeV $\text{O}^{8+} + \text{C}$	35 MeV $\text{O}^{7+} + \text{C}$	40 MeV $\text{F}^{9+} + \text{C}$	40 MeV $\text{F}^{8+} + \text{C}$
<i>VV</i> → <i>KK</i>	3993		4333	
<i>VK</i> → <i>KK</i>	3716		4056	
<i>KK</i> → <i>KK</i>	3439		3779	
<i>VV</i> → <i>KL</i>	3420	3244	3615	3414
<i>VK</i> → <i>KL</i>	3143	2967	3338	3137
<i>KK</i> → <i>KL</i>	2866	2690	3061	2859

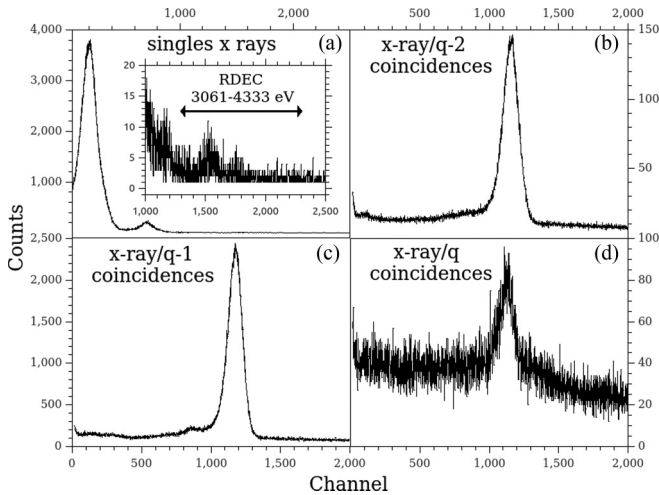


FIG. 3. Spectra for the 2.11 MeV/u $F^{9+} + C$ collision system showing (a) the singles x-ray spectrum and (b)–(d) the coincidence spectra between x rays and the outgoing charge states for q-2, q-1, and q, respectively. Similar spectra were obtained for F^{8+} , O^{8+} , and O^{7+} incident ions.

and the peak at about channel 700 is due to REC. At still higher channel numbers, in the range from ~ 1300 – 2300 , lie the expected RDEC events that cannot be seen due to the noise counts in that region (the peaks centered near channels 1500 and 1750 are due to contamination, to be discussed below). The peaks occurring in the q-2, q-1, and q x-ray/particle spectra [panels (b)–(d)] result from coincidences between x rays and the particles. Similar spectra were recorded (not shown) for the other three target-projectile systems studied. These spectra can be used to generate x-ray-gated particle spectra and particle-gated x-ray spectra.

Figure 4 shows the x-ray-gated particle spectra for fully stripped [panels (a)–(c)] and one-electron [panels (e)–(g)] fluorine projectile ions. These spectra were produced by applying a gate in the RDEC region of the x-ray spectrum [see Fig. 3(a)]. Peaks were observed for all three outgoing charge states and the number of events associated with the spectra due to RDEC are shown in each panel. Panels (d) and (h) show the particle-gated x-ray spectra summed for the three outgoing charge states q-2, q-1, and q for F^{9+} and F^{8+} , respectively. In these spectra, contributions from contamination in the RDEC region with peaks centered near 3.4 and 3.8 keV are seen. These peaks are attributed to potassium and calcium. Similar peaks were also seen in the earlier data taken for $F^{9+} + C$ collisions [3].

Figure 5 shows the x-ray-gated particle spectra, produced by applying a gate to the RDEC region of the singles x-ray spectrum in a manner similar to that of Fig. 4, for incident fully stripped [panels (a)–(c)] and one-electron [panels (e)–(g)] oxygen-projectile ions. Again, peaks are observed in these spectra (except the q-2 and q-1 spectra for O^{7+}) and the counts associated with each of the peaks are listed in the panels. Examination of the spectra indicates a significant shift to higher relative outgoing charge states compared to $F^{9,8+}$ despite these two species being just one atomic number apart. Specifically, for incident fully stripped O^{8+} there are very few counts in the q-2 spectrum compared to F^{9+} where

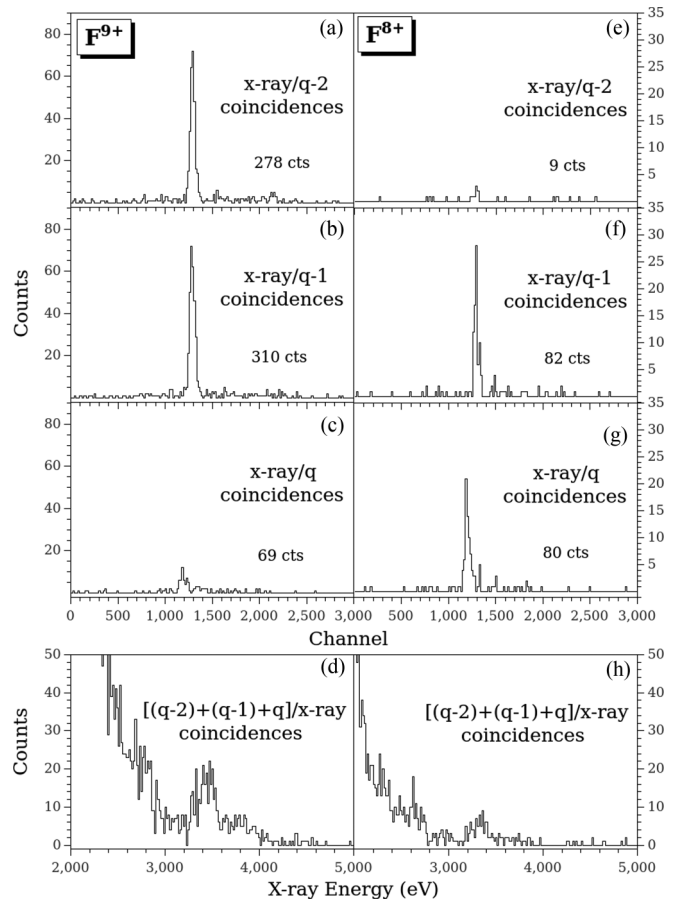


FIG. 4. Panels (a), (b), and (c) show the x-ray-gated particle spectra for the doubly charge changed (q-2), singly charge changed (q-1), and no charge changed (q) states for 2.11 MeV/u $F^{9+} + C$, respectively. Panels (e), (f), and (g) show the same information for the outgoing charge states of the $F^{8+} + C$ collision system. Panels (d) and (h) show the summed particle-gated x-ray spectra for the q-2, q-1, and q outgoing charge states of F^{9+} and F^{8+} , respectively. The total number of incident projectiles for F^{9+} was 7.13×10^9 , while it was 2.48×10^9 for F^{8+} .

many counts were observed, as expected. For O^{7+} , there are no counts in the q-2 spectrum while there are a few counts in this spectrum for F^{8+} . The fact that there are essentially no RDEC counts in the q-2 or q-1 spectra of O^{7+} indicates that captured electrons are lost before the charge-changed particles reach the analyzing magnet where they are recorded by the q particle detector. Hence, RDEC transitions in which one of the captured electrons must initially be in the L shell have a higher probability of the projectile losing one of these electrons as it passes through the foil. This implies larger charge-stripping cross sections for O^{7+} ions compared to F^{8+} at these energies (see Refs. [12–14], discussed below).

For these ions incident on gas targets this does not occur, with the RDEC events occurring instead only in the q-2 outgoing channel, as expected (see Ref. [1], Figs. 2 and 3). The outcome in the present work is attributed to multiple charge-changing collisions occurring inside the foil following RDEC events taking place earlier in the foil. The variations between the projectiles and charge states is due primarily to differences in the electron-loss cross sections for the two

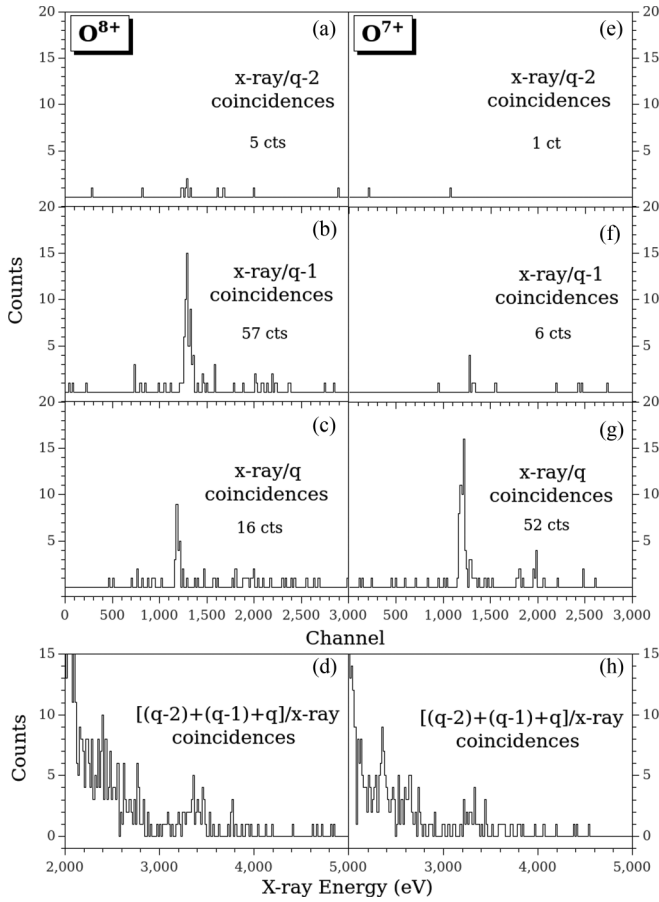


FIG. 5. Panels (a), (b), and (c) show the x-ray-gated particle spectra for the doubly charge changed (q-2), singly charge changed (q-1), and no charge changed (q) states for 2.19 MeV/u $O^{8+} + C$, respectively. Panels (e), (f), and (g) show the same information for the outgoing charge states of the $O^{7+} + C$ collision system. Panels (d) and (h) show the summed particle-gated x-ray spectra for the q-2, q-1, and q outgoing charge states of O^{8+} and O^{7+} , respectively. The total number of incident projectiles for O^{8+} was 3.74×10^9 , while for O^{7+} it was 2.11×10^9 .

projectiles and charge states studied, which can be seen from Table II [12–14]. Shown in the table are the estimated single-stripping cross sections for oxygen and fluorine projectiles striking a thin-carbon foil. By multiplying the cross sections given by half the foil thickness (on average the beam passes through half the foil following an RDEC event), the relative

TABLE II. Estimated charge-stripping cross sections for ~ 2 MeV/u O^{q+} and F^{q+} on carbon. The O^{q+} and F^{q+} cross sections were scaled from Refs. [12,13] and Ref. [14], respectively. By applying the cross sections to the relevant charge states of Figs. 4 and 5, the relative distributions of the q-2, q-1, and q spectra can be readily seen.

$O^{q+} + C$	Cross sec. (Mb)	$F^{q+} + C$	Cross sec. (Mb)
$5+ \rightarrow 6+$	19.0	$6+ \rightarrow 7+$	4.0
$6+ \rightarrow 7+$	3.6	$7+ \rightarrow 8+$	1.0
$7+ \rightarrow 8+$	0.4	$8+ \rightarrow 9+$	0.2

distributions of x-ray/particle coincidences seen in Figs. 4 and 5 are readily confirmed. Hence, for foil targets this exhibits the necessity to measure coincidences between x rays and all of the possible outgoing charge states. If this is not done, the correct value of the cross sections cannot be attained.

Another difference to note between the present spectra and those recorded in the earlier work for oxygen projectiles [2] is the fact that the RDEC events seen in the present work for fully stripped and one-electron oxygen ions are comparable in magnitude. This finding is very different from Ref. [2], in which it was reported that RDEC did not occur for the one-electron projectiles. The reason for this can be found in Fig. 5. There, it is seen that for fully stripped ions RDEC occurs in the q-2 (expected, but small) and q-1 channels (most of the events occur here), with some events in the q channel. However, for the one-electron projectile, Fig. 5 shows that nearly all of the RDEC events are in the q channel, results that can be attributed to the larger electron-loss cross sections for O^{7+} [12–14]. In recording the data for Ref. [2], coincidences with the q channel were not measured as it was unexpected that RDEC would appear for this charge state. It is also noted that stripping of the O^{7+} might occur prior to an RDEC event, but the probability of this is very small due to the relatively large stripping cross section (approximately megabarns) and the very small RDEC cross section (approximately barns). Hence, this possibility does not have to be considered.

Another consideration is the probability that the charge distribution for RDEC is not in equilibrium as has been observed for REC events [15]. However, the foil thickness in the present work is near the beginning of the curve (thickness ~ 0) where the cross section obtained is equal to the desired value when the charge has not changed appreciably (see Fig. 3 of Ref. [15]). Hence, this possibility does not need to be considered, and the small difference from equilibrium can be taken into account in the overall uncertainties assigned to the cross sections.

To determine the RDEC cross sections corresponding to each projectile charge state and target, the contamination due to the x-ray lines observed near 3.4 and 3.8 keV [Figs. 4(d) and 4(h) and 5(d) and 5(h)] must be corrected for. The origin of these lines is not understood, but they have been observed before in our measurements for fluorine ions [3]. They might have come from improper handling of the foils prior to their installation in the target chamber. Corrections for the contaminant lines was done by generating additional x-ray-gated particle spectra (not shown) corresponding to a region encompassing these two peaks (from about 3.3 to 4.0 keV). Recognizing that subtracting the full contribution of the contaminant lines would consequently underestimate the actual cross sections, the counts subtracted were adjusted, leaving one-third of the contaminant contribution in the RDEC cross section. The uncertainty in making this correction has been included in determining the error bars for the cross sections.

The data of Figs. 4 and 5 also show large differences in the relative number of counts for the various projectiles and charge states that were observed. While the absolute numbers shown are largely due to variations in the total number of incident particles recorded for each projectile, the relative differences cannot be ascribed to these absolute numbers.

TABLE III. Calculated total RDEC cross sections (b/atom) for the four projectile-target systems investigated. The cross sections shown have been corrected for the K and Ca contaminant peaks observed in Figs. 4(d) and 4(h) and 5(d) and 5(h).

σ_{total}	Projectile-target system			
	$\text{O}^{8+} + \text{C}$	$\text{O}^{7+} + \text{C}$	$\text{F}^{9+} + \text{C}$	$\text{F}^{8+} + \text{C}$
	2.0 ± 0.4	2.9 ± 0.5	7.9 ± 1.4	6.2 ± 1.0

These differences are taken into account in calculating the cross section for each projectile and charge state.

Since only the differential cross sections at 90° were measured in this work, an angular dependence of $\sin^2 \theta$ between the differential and total cross sections was assumed (see Refs. [16,17]). The total cross sections were therefore calculated by multiplying the differential cross sections by $8\pi/3$, giving the RDEC cross sections for the four projectile-target systems listed in Table III.

The RDEC cross section for one-electron fluorine (F^{8+}) is smaller by about 20% compared to that of fully stripped fluorine (F^{9+}). Typically, this would be attributed to the fact that RDEC transitions ending with both electrons in the *K* shell, i.e., *KK* transitions, are not possible for F^{8+} . However, this does not hold for oxygen projectiles, for which the results show the O^{7+} ion to have a cross section larger than that for O^{8+} . The present value for O^{8+} is more than two times smaller than that found in Ref. [2], while the F^{9+} value is only marginally smaller than that reported in Ref. [3]. These results for $\text{F}^{9,8+}$ and $\text{O}^{8,7+}$ projectiles incident on thin-foil C targets indicate probabilities for RDEC transitions ending in the *KK* and *KL* states are more comparable than those found for $\text{F}^{9,8+}$ projectiles on gas targets of N_2 and Ne, for which the difference was a factor of about 6. In Ref. [2] no RDEC was reported for O^{7+} projectiles, but it should be noted that in the present work only coincidences with the charge state of the main beam were observed for this projectile [see Fig. 5(g)] while these coincidences were not measured in Ref. [2].

The cross sections from Table III are plotted in Fig. 6. The left panel shows the cross sections as solid circles determined for the four projectile-target systems in the present work, along with the cross sections reported in the previous C-foil experiments (solid squares) [2,3]. The most recent theoretical cross sections [11] are shown with the open square and circular symbols. The theoretical cross sections were calculated using the line-profile approach by two methods labeled as the *A* model and *K* model in the figure. In the *A* model, a homogeneous electron density was assumed for the entire target atom and all the electrons were taken into account. In the *K* model, only the target *K* electrons were considered and a homogeneous electron density was assumed for the *K* shell. The theoretical values disagree substantially with the measured values, with the results of the *A* model being the closest. Other theoretical calculations [18–20] show poorer agreement with the data and are not included in this analysis.

The right panel in Fig. 6 shows the RDEC cross sections obtained for fluorine projectiles with the gas targets N_2 and Ne in measurements done at Western Michigan University [1].

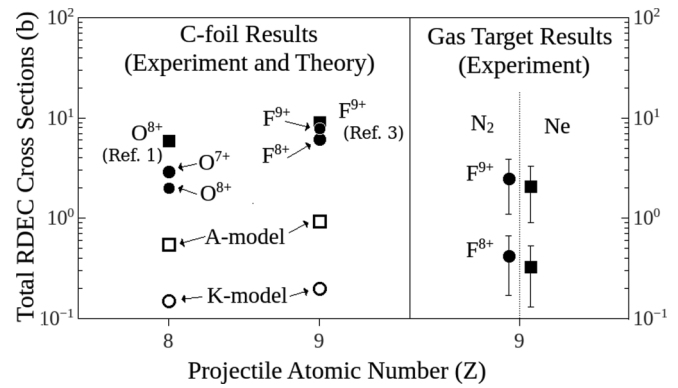


FIG. 6. Total RDEC cross sections determined from the current measurements compared with previous experiments and theoretical values. The left panel shows the cross sections (experimental and theoretical) for oxygen and fluorine projectiles in collisions with thin carbon-foil targets and the right panel shows previous experimental RDEC cross sections for fluorine projectiles in collisions with gas targets of N_2 and Ne [1].

The solid circles represent the cross sections obtained with the N_2 target while the solid squares represent cross sections obtained for the Ne target. No theoretical calculations yet exist for these gas targets. The cross sections for the gas targets are substantially lower than those for the C-foil target, and, furthermore, the cross sections for the fully stripped ions differ by a factor of nearly 6 from the cross sections for the one-electron ions. This significant difference between the fully stripped and one-electron ions needs further investigation.

The cross sections for fully stripped oxygen and fluorine ions determined from the present measurements agree fairly well with the previous values, but in all cases are smaller. In the present work, cross sections for the C-foil target are reported with one-electron projectile ions. These cross sections do not differ greatly from those for the bare ions, contrary to the results previously found for F^{9+} and F^{8+} ions on gas targets under single collision conditions where the difference was about a factor of 6. This large contrast is attributed to the effect of multiple collisions for the projectile ions incident on thin-carbon foils. Understanding these differences would benefit greatly from additional theoretical cross sections to shed more light on the RDEC process under both single- and multiple-collision conditions.

In summary, RDEC was investigated and observed for fully stripped and one-electron $\text{O}^{8,7+}$ and $\text{F}^{9,8+}$ ions incident on thin-foil C targets. The RDEC cross sections for fluorine ions are larger by factors of about 2–4 compared to those for oxygen. The cross sections are found to vary considerably with the charge state of the *outgoing* projectile, with the maximum RDEC cross section occurring one charge state higher for F^{8+} compared with F^{9+} , and likewise for the oxygen projectiles. The same is true when oxygen is compared with fluorine, with the oxygen projectiles showing little intensity in the expected *q*-2 *outgoing* charge state. The total RDEC cross sections found for fluorine ions striking the C-foil target are about twice the size of those found for N_2 and Ne targets for incident fluorine.

Multiple charge-changing collisions have a large influence on RDEC for foil targets, while for gas targets RDEC involves single collisions. The multiple collisions thus require more extensive measurements with more difficult analyses. The experimental cross sections are larger than those predicted by Mistonova and Andreev [11] and are likely due to assumptions (mentioned above) made in their *A*-model and *K*-model

theories to simplify the calculations. With these measurements, the experimental situation of the cross sections becomes clearer but the agreement with the best theory is still not good, thus requiring more work.

This work was supported in part by National Science Foundation Grant No. PHY-1707467.

-
- [1] D. S. La Mantia, P. N. S. Kumara, S. L. Buglione, C. P. McCoy, C. J. Taylor, J. S. White, A. Kayani, and J. A. Tanis, *Phys. Rev. Lett.* **124**, 133401 (2020).
- [2] A. Simon, A. Warczak, T. ElKafrawy, and J. A. Tanis, *Phys. Rev. Lett.* **104**, 123001 (2010).
- [3] T. ElKafrawy, A. Simon, J. A. Tanis, and A. Warczak, *Phys. Rev. A* **94**, 042705 (2016).
- [4] A. Warczak *et al.*, *Nucl. Instrum. Methods Phys. Res., Sect. B* **98**, 303 (1995).
- [5] G. Bednarz *et al.*, *Nucl. Instrum. Methods Phys. Res., Sect. B* **205**, 573 (2003).
- [6] N. Winters *et al.*, *Phys. Scr.* **T156**, 014048 (2013).
- [7] A. V. Nefiodov, A. I. Mikhailov, and G. Plunien, *Phys. Lett. A* **346**, 158 (2005).
- [8] J. Miraglia and M. S. Gravielle, *International Conference on Photonic, Electronic and Atomic Collisions XV: Book of Abstracts* (Springer, Boston, 1987), p. 517.
- [9] H. W. Schnopper, H. D. Betz, J. P. Delvaille, K. Kalata, A. R. Sohval, K. W. Jones, and H. E. Wegner, *Phys. Rev. Lett.* **29**, 898 (1972).
- [10] T. Stöhlker *et al.*, *Phys. Rev. A* **51**, 2098 (1995).
- [11] E. A. Mistonova and O. Y. Andreev, *Phys. Rev. A* **87**, 034702 (2013).
- [12] T. R. Dillingham, J. R. Macdonald, and P. Richard, *Phys. Rev. A* **24**, 1237 (1981).
- [13] S. A. Boman, E. M. Bernstein, and J. A. Tanis, *Phys. Rev. A* **39**, 4423 (1989).
- [14] S. M. Ferguson, J. R. Macdonald, T. Chiao, L. D. Ellsworth, and S. A. Savoy, *Phys. Rev. A* **8**, 2417 (1973).
- [15] J. A. Tanis and S. M. Shafroth, *Phys. Rev. Lett.* **40**, 1174 (1978).
- [16] R. Anholt *et al.*, *Phys. Rev. Lett.* **53**, 234 (1984).
- [17] S. Tashenov, T. Stöhlker, D. Banas, K. Beckert, P. Beller, H. F. Beyer, F. Bosch, S. Fritzsche, A. Gumberidze, S. Hagmann *et al.*, *Phys. Rev. Lett.* **97**, 223202 (2006).
- [18] V. L. Yakhontov and M. Y. Amusia, *Phys. Lett. A* **221**, 328 (1996).
- [19] V. L. Yakhontov and M. Y. Amusia, *Phys. Rev. A* **55**, 1952 (1997).
- [20] A. I. Mikhailov, I. A. Mikhailov, A. N. Moskalev, A. V. Nefiodov, G. Plunien, and G. Soff, *Phys. Rev. A* **69**, 032703 (2004).